

# Antiproliferative Activity and Apoptotic Mechanisms of $\beta$ -Sitosterol and Its Derivatives as Anti-Breast Cancer Agents: In Silico and In Vitro

Mutakin Mutakin<sup>1</sup>, Lauren Pangestu<sup>2</sup>, Nafisa Nurfatma Hidayat<sup>2</sup>, Fajar Fauzi Abdullah<sup>3</sup>, Yuni Elsa Hadisaputri<sup>2</sup>

<sup>1</sup>Department of Pharmaceutical Analysis and Medicinal Chemistry, Faculty of Pharmacy, Universitas Padjadjaran, West Java, Indonesia; <sup>2</sup>Department of Pharmaceutical Biology, Faculty of Pharmacy, Universitas Padjadjaran, West Java, Indonesia; <sup>3</sup>Department of Chemistry, Faculty of Mathematics and Natural Science, Universitas Garut, West Java, Indonesia

Correspondence: Mutakin Mutakin, Department of Pharmaceutical Analysis and Medicinal Chemistry, Faculty of Pharmacy, Universitas Padjadjaran, Jl. Raya Bandung-Sumedang KM.21, Jatinangor, West Java, 45363, Indonesia, Tel +62-22-84288888 Ext. 3510, Email mutakin@unpad.ac.id

**Introduction:** Breast cancer has become the most frequently diagnosed cancer worldwide. Beta-sitosterol and its derivatives have been explored for its anticancer properties. Therefore, this study aims to analyze the testing procedure carried out on MCF7 and MDA-MB-231 breast cancer cells, as well as MCF 10A non-cancerous breast epithelial cells.

**Methods:** The compounds tested included  $\beta$ -sitosterol and its derivatives: 3 $\beta$ -galactose sitosterol, sitostenone, 3 $\beta$ -glucose sitosterol, poriferasta-5, 22E, 25-trien-3 $\beta$ -ol, and 22-dehydrocholesterol. Cytotoxicity assay was conducted using the PrestoBlue™ Cell Viability Reagent on MCF-7, MDA-MB-231, and MCF 10A cells. The compounds with the highest and lowest cytotoxicity were further analyzed for their mechanisms of action through cell morphology assessments and molecular docking studies. mRNA expression levels were also evaluated to confirm the findings.

**Results:** The results showed that 3 $\beta$ -glucose sitosterol exhibited the most promising cytotoxic activity with IC<sub>50</sub> values against MCF7, MDA-MB-231 breast cancer cells, and MCF 10A non-cancerous cells of 265  $\mu$ g/mL, 393.862  $\mu$ g/mL, and 806.833  $\mu$ g/mL, respectively. Molecular docking simulations showed that the compound is bound to estrogen receptor beta and caspase-3, suggesting a potential mechanism of action as evidenced by the best binding energy of -6.94 kcal/mol and inhibition constant values of 8.16  $\mu$ M. Furthermore, gene expression analysis confirmed the induction of apoptosis through the upregulation of *caspase-9* and *caspase-3* mRNA expression.

**Conclusion:** Based on the results,  $\beta$ -sitosterol and its derivatives, particularly 3 $\beta$ -glucose sitosterol, show as the most promising potential adjuvant therapy for hormone-positive breast cancer.

**Keywords:**  $\beta$ -sitosterol, 3 $\beta$ -glucose sitosterol, breast cancer, MCF7, MDA-MB-231, ESR2

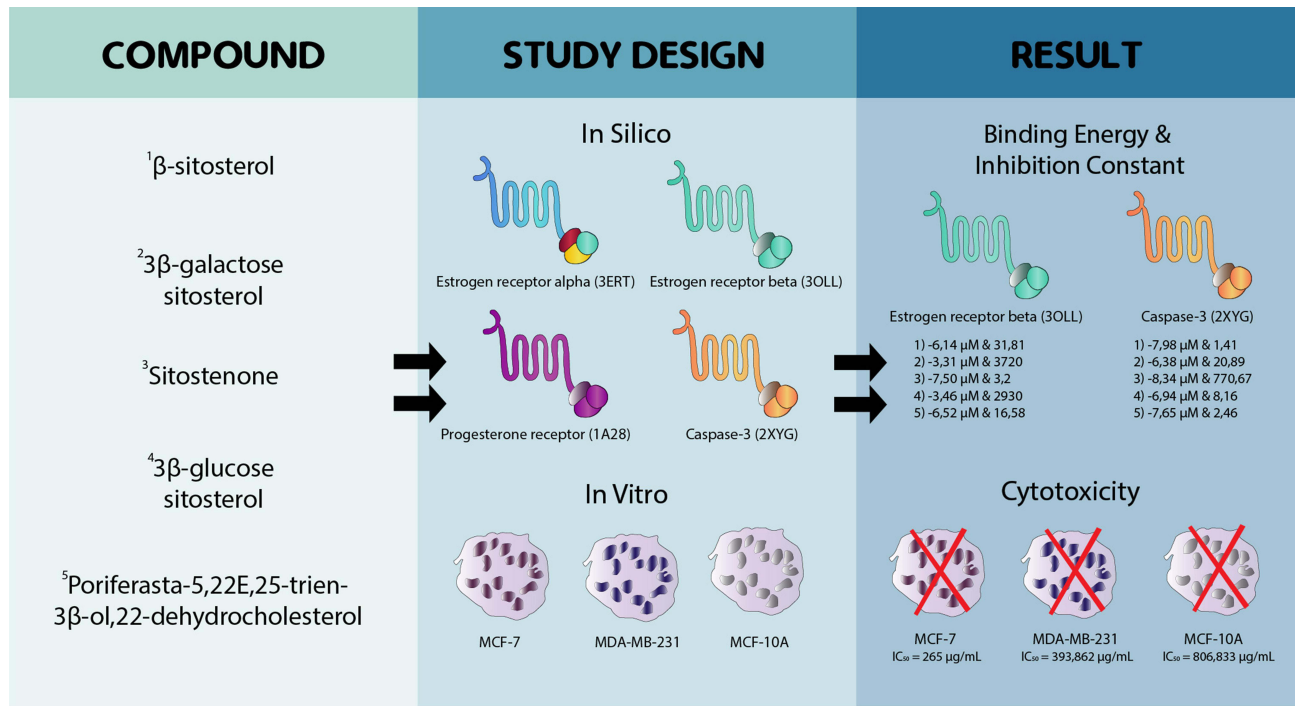
## Introduction

Cancer is a non-communicable disease characterized by the uncontrolled proliferation of cells to nearby tissues or organs.<sup>1</sup> According to the WHO, the disease is one of the most common causes of death worldwide. Breast cancer has surpassed lung cancer as the most frequently diagnosed worldwide, with 2.3 million new cases (11.6%). In Indonesia, this cancer also has the highest number of cases. In the Global Cancer Observatory (GLOBOCAN) 2022 report, Indonesia recorded 66,271 new cases out of a total of 408,661 breast cancer, resulting in over 22,000 deaths.<sup>2</sup>

There are several types of treatment for breast cancer, namely local therapy through surgery and systemic chemotherapy, which is the oral or intravenous administration of anticancer drugs. Surgery is adopted in early-stage cancer cases where the disease has not metastasized, while chemotherapy drugs may be used in early or advanced stages.<sup>3</sup>

These drugs provide a strong effect and are unable to properly differentiate between cancerous and non-cancerous tissues. Therefore, non-cancerous cells with rapid division can also be attacked, such as bone marrow cells, hair cells, skin,

Graphical Abstract



mouth, and digestive tract.<sup>4</sup> The development of chemotherapy is focused on finding new drugs, including compounds isolated from nature considered safer and more selective to target cancer tissue without damaging healthy cells.

MCF-7 is a human breast cancer cell line that expresses estrogen, progesterone, and glucocorticoid receptors, making it important for in vitro studies. It is the first hormone-responsive breast cancer cell line and is prevalent among women.<sup>5</sup> The MDA-MB-231 cell line, representing late-stage breast cancer, corresponds to the basal subtype, lacks HER2, and is a model for triple-negative breast cancer, showing invasive traits in vitro.<sup>6</sup>

Beta-sitosterol is one of the most abundant phytosterols, and the compound has different pharmacological activities, such as anti-inflammatory, antibacterial, antifungal, antidiabetic, antioxidant, and anti-cancer. Several previous studies have reported that the compound possessed toxic properties in T47D breast cancer cell line, HeLa cervical cancer cell line, HepG2 liver cancer cell line, and lung cancer cell line A549.<sup>7,8</sup>

Among the β-sitosterol derivatives, Sitostenone demonstrated notable cytotoxicity with an IC<sub>50</sub> value of 128.11 μM against the MDA-MB-231 breast cancer cell line.<sup>9</sup> This suggests that structural modifications can enhance the anticancer potential of β-sitosterol. Further exploration of other derivatives such as 3β-galactose sitosterol, 3β-glucose sitosterol, and Poriferasta-5,22E,25-trien-3β-ol,22-dehydrocholesterol were not reported yet, and it is necessary to evaluate their cytotoxic profiles and mechanisms of action.

The efficacy of β-sitosterol and derivatives is considered promising as an anticancer drug with significant effects.<sup>10</sup> The cytotoxic activities of the compounds were assessed on MCF7 breast cancer and MCF 10A epithelial cell line using PrestoBlue assay method. Moreover, Polymerase Chain Reaction (PCR) and molecular docking simulations were performed to determine the molecular mechanism of β-sitosterol and its derivatives. This study aims to expand upon previous research and analyze the testing procedure carried out on MCF7 and MDA-MB-231 breast cancer cells, as well as MCF 10A non-cancerous breast epithelial cells as potent anticancer agents.

## Materials and Methods

### Materials

The compounds used in this research were beta-sitosterol and derivatives, including 3 $\beta$ -galactose sitosterol, sitostenone, 3 $\beta$ -glucose sitosterol, and poriferasta-5,22E,25-trien-3 $\beta$ -ol,22-dehydrocholesterol. Beta-sitosterol from *Annona muricata*,<sup>11</sup> 3 $\beta$ -galactose sitosterol and 3 $\beta$ -glucose sitosterol from *Azadirachta indica*,<sup>12</sup> Sitostenone from *Toona ciliata*,<sup>13</sup> and Poriferasta-5,22E,25-trien-3 $\beta$ -ol,22-dehydrocholesterol from *Clerodendrum paniculatum*<sup>14</sup> were dissolved in dimethyl sulfoxide (DMSO) and growth medium to make a 250  $\mu$ g/mL stock solution. Subsequently, MCF 10A human breast epithelial cells was obtained from the American Type Culture Collection (ATCC, Manassas, VA, USA), while MCF7 primary invasive ductal carcinoma cells, and MDA-MB-231 adenocarcinoma cells were obtained from the European Collection of Authenticated Cell Cultures (ECACC, Salisbury, United Kingdom).

### Cytotoxic Test on MCF7 Breast Cancer Cells and MCF10A Epithelial Cells

The cytotoxicity of the compounds was assessed using the PrestoBlue assay method. MCF7 cells obtained from ECACC were grown in Eagle's Minimum Essential Medium/EMEM (Sigma Aldrich; Merck KGaA, Darmstadt, Germany) liquid culture medium containing 10% fetal bovine serum (FBS) (Gibco, Grand Island, NY, USA) and 1% penicillin-streptomycin (Gibco). Meanwhile, MCF 10A cells were grown on Mammary Epithelial Cell Basal Medium/MEBM (Lonza, Basel, Switzerland) to 70–80% confluency. In addition, the cells were distributed at a density of 10,000 cells/well into 96-well plates and incubated for 24 h at 37°C and 5% CO<sub>2</sub> gas. Treatment was then conducted with eight concentration series of samples, namely 250  $\mu$ g/mL, 125  $\mu$ g/mL, 62.5  $\mu$ g/mL, 31.25  $\mu$ g/mL, 15.625  $\mu$ g/mL, 7.8125  $\mu$ g/mL, 3.9  $\mu$ g/mL, and 1.95  $\mu$ g/mL for 24 h. In this context, the concentration of the compounds was tested in three parallel experiments. Cisplatin was used as a positive control in this test. The wells containing only culture media served as media controls, while those without a compound served as cell, DMSO, and positive controls. After overnight incubation, 10  $\mu$ L of PrestoBlue™ reagent (Thermo Fisher Scientific, Waltham, Massachusetts, USA) was added to each well and re-incubated for 2 h until a color change was reported. The intensity of the color changes was read using a microplate reader Infinite M200 PRO multimode (Tecan, Männedorf, Switzerland) at 570 nm and 600 nm (reference wavelength). From the measurement results, the percentage of cell growth inhibition was calculated using the equation.<sup>15</sup>

$$\% \text{ Cell Inhibition} = 100 - \left( \frac{\text{Absorbance of test} - \text{Absorbance of blank}}{\text{Absorbance of control} - \text{Absorbance of blank}} \right) \times 100\%$$

IC<sub>50</sub> values were calculated by linear regression method using Microsoft Excel software.

### Molecular Docking

Molecular docking was carried out to analyze the binding mode of compounds in the active site of estrogen and progesterone receptors. The three-dimensional crystal structure of the receptors (PDB ID: 3ERT (ER $\alpha$ ), 3OLL (ER $\beta$ ), 1A28 (PR)) was downloaded from the Protein Data Bank (PDB). In addition, proteins were prepared by removing water molecules and native ligands using BIOVIA Discovery Studio software. A re-docking process of the native ligand with each receptor was performed and succeeded with RMSD values <2Å to evaluate the accuracy of docking. The preparation was carried out with energy minimization in 3D structures using Chem3D Pro 12.0 software (PerkinElmer, Inc., Shelton, Connecticut, USA). Compounds were docked into the active site of protein using AutodockTools 1.5.6 software (Center for Computational Structural Biology, San Diego, California, USA) (Grid box 40  $\times$  40  $\times$  40). At the end of the process, the predicted ligand-protein complexes were analyzed using BIOVIA Discovery Studio software (San Diego, California, USA).

### RNA Extraction and PCR

MCF7 cells were seeded at a density of 100.000 cells/well in a 12-well cell culture plate. The cells were exposed to each compound at different time points, namely 0, 12, and 24 h. Subsequently, RNA was isolated using the innuPREP DNA/RNA Mini Kit (Analytik Jena, Thuringia, Germany). The purity was also assessed by measuring the A260/A280 ratio using an Infinite M200 PRO multimode microplate reader (Tecan) and a GelPilot® DNA loading dye kit (Qiagen, Hilden, Germany). The mRNA expression was measured using PCR with designed primers in Table 1 and the *GAPDH* gene was

**Table 1** Primers That Were Used in This Research

Primer		Sequences	T* (°C)
<i>caspase-9</i>	Forward	5'-AAGTGACCCTCCCAAGTAGC-3'	60.5
	Reverse	5'-GTTCTGGCCAGGTCTCTTCT-3'	
<i>caspase-3</i>	Forward	5'-AAAATACCAGTGGAGGCCGA-3'	58.4
	Reverse	5'-GCACAAAGCGACTGGATGAA-3'	
<i>PARP-1</i>	Forward	5'-TGGAACATCAAGGACGAGCT-3'	60.5
	Reverse	5'-CATCGCTCTTGAAGACCAGC-3'	
<i>Bcl-2</i>	Forward	5'-TCCTCTTTACTGTCAGG-3'	60.5
	Reverse	5'-GAGTATTTGTGACGAGGG-3'	
<i>PR-AB</i>	Forward	5'-TGGAAGAAATGACTGCATCG-3'	58
	Reverse	5'-AGCATCCAGTGTCTCACAA -3'	
<i>ESR2</i>	Forward	5'-CAATGCATATCCTGCCTGTG-3'	60
	Reverse	5'-TCCCGGAAATCTGATACAGC-3'	
<i>GAPDH</i>	Forward	5'-AAGGTGAAGGTCGGAGTCAAC-3'	57.3
	Reverse	5'-CTTGATTTGGAGGGATCTCG-3'	

used as an internal control (Macrogen, Seoul, South Korea). Each reaction contained 12.5  $\mu$ L MyTaq One-Step mix (Meridian Bioscience, Hamilton, Newton, USA), 0.25  $\mu$ L Reverse transcriptase, 0.5  $\mu$ L RiboSafe RNase Inhibitor, 10  $\mu$ L forward primer, 10  $\mu$ L reverse primer, 5  $\mu$ L RNA template, and DEPC H<sub>2</sub>O up to 25  $\mu$ L. In addition, PCR amplification was conducted through 40 cycles, under specific conditions of reverse transcription and polymerase activation at 45°C and 95°C for 20 and 1 min, respectively. The reaction was repeated at 95°C, 59.5°C–62.5°C, and 72°C for denaturation, primer attachment, and extension, respectively. Electrophoresis was performed to quantify the result of PCR products, and the expression levels of the target genes were analyzed using ImageJ software (NIH, Bethesda, MD, USA).

## Statistical Analysis

The quantitative data of protein and mRNA expression were measured using ImageJ 1.53v (NIH) in triplicate. The normality of the data was obtained by a stem and leaf plot, while the statistical significance was calculated through one-way ANOVA and Tukey's post hoc test for homogen distribution and Mann–Whitney *U*-test. The differences between the data were considered statistically significant when the P-value was <0.05 and the assessment was performed using IBM SPSS statistic 26 (IB Corp., NY, USA).

## Results

### Cytotoxic Activity by $\beta$ -Sitosterol and the Derivatives

MCF7 and MDA-MB-231 were compared with the epithelial breast cell MCF 10A to confirm the cytotoxic activity of  $\beta$ -sitosterol and the derivatives against breast cancer. The inhibition concentration of 50% cell death (IC<sub>50</sub>) value of  $\beta$ -sitosterol as base structure compound against MCF 10A, MCF7, and MDA-MD-231 was 232.534  $\mu$ g/mL, 187.61  $\mu$ g/mL, and 874.156  $\mu$ g/mL, respectively. In addition, 3 $\beta$ -galactose sitosterol was a derivative of  $\beta$ -sitosterol with an IC<sub>50</sub> value of 734.92  $\mu$ g/mL, 609.66  $\mu$ g/mL, and 907.464  $\mu$ g/mL against MCF 10A, MCF7, and MDA-MD-231, respectively. In contrast, the results of Sitostenone with IC<sub>50</sub> value against MCF 10A, MCF7, and MDA-MD-231 were 106.19  $\mu$ g/mL, 168.52  $\mu$ g/mL, and 194.88  $\mu$ g/mL, respectively. The IC<sub>50</sub> value of 3 $\beta$ -glucose sitosterol against MCF 10A, MCF7, and MDA-MD-231 was 806.833  $\mu$ g/mL, 265  $\mu$ g/mL, and 393.65  $\mu$ g/mL. Additionally, the IC<sub>50</sub> value of Poriferasta-5,22E,25-trien-3 $\beta$ -ol,22-

**Table 2** Inhibition Concentration of 50% Cell Death (IC<sub>50</sub>) Value of  $\beta$ -Sitosterol and the Derivatives

Compound	IC <sub>50</sub> Value ( $\mu$ g/mL)		
	MCF 10A	MCF7	MDA-MB-231
$\beta$ -sitosterol	232,534	187,61	874,156
3 $\beta$ -galactose sitosterol	734,92	609.66	907,464
Sitostenone	106,193	168,52	194,884
3 $\beta$ -glucose sitosterol	806,833	265	393,652
Poriferasta-5,22E,25-trien-3 $\beta$ -ol,22-dehydrocholesterol	653,37	n.d.	130,165
Cisplatin	106,81	30,08	21,6

**Abbreviation:** n.d, not detected.

dehydrocholesterol against MCF 10A, MCF7, and MDA-MD-231 was 653.37  $\mu$ g/mL, more than 1000  $\mu$ g/mL (not detected), and 130.165  $\mu$ g/mL, while for control positive we used cisplatin with IC<sub>50</sub> value against MCF 10A, MCF7, and MDA-MB-231 was 106.81  $\mu$ g/mL, 30.08  $\mu$ g/mL, and 21.6  $\mu$ g/mL, respectively, as reported in Table 2.

The cellular morphology of MCF7 cells treated with  $\beta$ -sitosterol showed cell blebbing indicative of apoptotic process, which occurred in MCF10A and MCF7 cells, but to a lesser extent in MDA-MB-231 cells. The morphology of MCF7 cells treated with 3 $\beta$ -galactose sitosterol did not show differences with blebbing cells. Apoptotic process of MCF7 cells occurred in MDA-MB-231 but the observed morphology appeared similar to cells treated with  $\beta$ -sitosterol. Additionally, the occurrence of apoptotic process was observed in MCF10A cells treated with sitostenone. Another  $\beta$ -sitosterol derivative, 3 $\beta$ -glucose sitosterol, induced apoptosis better than MCF7 cells. In this context, MCF7 and MDA-MB-231 cells treated with Poriferasta-5,22E,25-trien-3 $\beta$ -ol,22-dehydrocholesterol were subjected to apoptosis (Figure 1).

The choice of using *caspase-9* as a marker for apoptosis is particularly relevant because it plays a crucial role in the intrinsic apoptotic pathway. *Caspase-9* is activated in response to mitochondrial stress signals and is essential for executing programmed cell death by activating downstream effector caspases such as *caspase-3*. This intrinsic pathway is often triggered by various stimuli, including cellular stress and damage, which aligns with the observed morphological changes in the treated cell lines.

## The Binding of $\beta$ -Sitosterol and Derivatives Estimated by Molecular Docking

The molecular mechanisms within the breast cancer cells in MCF7 and MDA-MB-231 were determined. Since female hormones, such as estrogen and progesterone, also influence the occurrence of breast cancer, a simulation of the receptors was carried out. The results are shown in Table 3 ligand–receptor interactions are also shown in Figure 2.

This research examined 5 test ligands of  $\beta$ -sitosterol compounds tethered to 4 receptors 3ERT (Estrogen receptor alpha), 3OLL (Estrogen receptor beta), 1A28 (progesterone receptor), and 2XYG (Caspase-3). The  $\beta$ -sitosterol compound showed a strong binding energy to 3 OLL receptors (Estrogen receptor beta) with a value of  $-6.14$  kcal/mol and an inhibition constant of 31.81  $\mu$ M. In addition, it formed 3 alkyl bonds (ALA442, ILE441, and VAL438) with 2XYG having a binding energy of  $-7.98$  kcal/mol and an inhibition constant of 1.41  $\mu$ M. This compound formed alkyl bonds (TYR204, HIS121, CYS163, MET61) and 1 Pi-Sigma bond (PHE128). The remaining receptors showed positive binding energies with no inhibition constant and 3ERT formed 1 hydrogen bond (LEU 306). In the case of 3 $\beta$ -galactose sitosterol receptor 3OLL, the binding energy was  $-3.31$  kcal/mol with 2 alkyl (VAL438, ALA442) and 2 hydrogen (ILE446 and SER448) bonds. Meanwhile, the other 2 receptors showed positive binding energies, and no bonds were observed. The inhibition constant was only found in 3OLL, with a value of 3270  $\mu$ M. Receptor 2XYG also reported interactions with a binding energy value of  $-6.38$  kcal/mol, an inhibition constant of 20.89  $\mu$ M, as well as the formation of 2 conventional hydrogen bonds (THR59, GLU123), 1 carbon-hydrogen bond (GLY60), 1 Pi-Sigma bond (PHE256), and 3 Alkyl bonds (MET61, HIS121, TYR204). Similarly, sitostenone compound showed the highest binding energy against 3 OLL with a value of  $-7.50$  kcal/mol and an



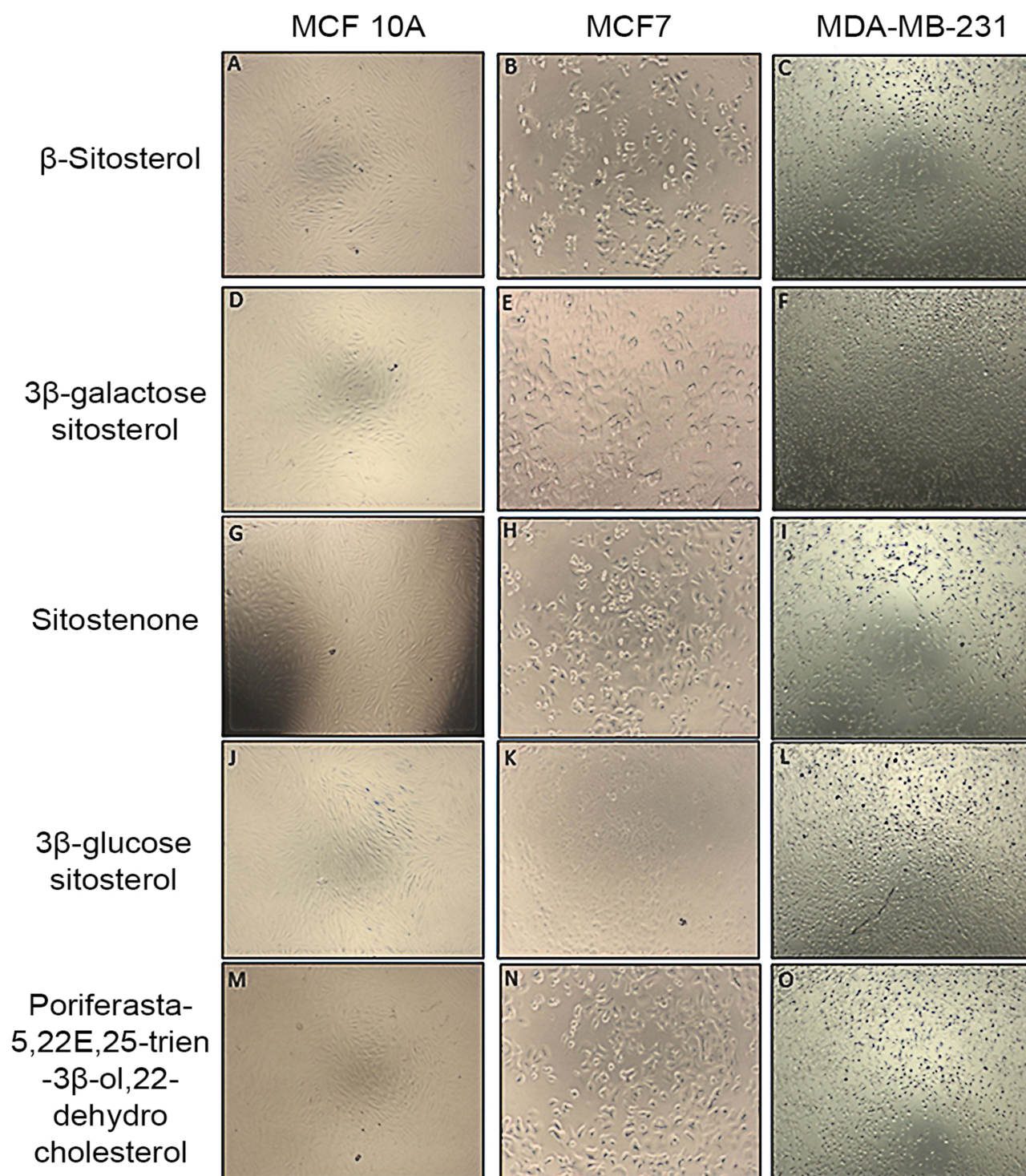


**Figure 1** Cell Morphology of MCF 10A, MCF7, and MDA-MB-231 after being treated with  $\beta$ -sitosterol and the derivatives. Beta-sitosterol against (A) MCF 10A, (B) MCF7, (C) MDA-MB-231, 3 $\beta$ -galactose sitosterol against (D) MCF 10A, (E) MCF7, (F) MDA-MB-231, Sitostenon against (G) MCF 10A, (H) MCF7, (I) MDA-MB-231, 3 $\beta$ -glucose sitosterol against (J) MCF 10A, (K) MCF7, (L) MDA-MB-231, Poriferasta-5,22E,25-trien-3 $\beta$ -ol,22-dehydrocholesterol against (M) MCF 10A, (N) MCF7, (O) MDA-MB-231.

inhibition constant of 3.2  $\mu$ M supported by the presence of 2 alkyl (VAL438, ALA 442) and 1 hydrogen bond (SER448). 2XYG receptor also reported a negative binding energy of  $-8.34$  kcal/mol, followed by an inhibition constant of 770.67  $\mu$ M, showing the presence of 5 bonds, namely, 1 conventional hydrogen bond (ARG207), 4 alkyl bonds (MET61, HIS121, TYR204, CYS163). In 3 $\beta$ -glucose sitosterol, 3OLL receptor formed 2 alkyl (VAL438, ALA A: 442) and 2 hydrogen bonds

**Table 3** Molecular Docking Result Data

Compound	Receptor	Cluster	Binding Energy (kcal/mol)	Ki (μM)	Bond
β-sitosterol	3ERT (Estrogen receptor alpha)	21	0.8	-	LEU306
	3OLL (Estrogen receptor beta)	15	-6.14	31.81	ALA442, ILE441, VAL438
	1A28 (Progesterone receptor)	7	2.09	-	-
	2XYG (Caspase-3)	1	-7.98	1.41	TYR204 HIS121 CYS163 MET61 PHE128
3β-galactose sitosterol	3ERT (Estrogen receptor alpha)	13	3.23	-	-
	3OLL (Estrogen receptor beta)	2	-3.31	3720	ALA442, ILE446, VAL438, SER448
	1A28 (Progesterone receptor)	2	3.88	-	-
	2XYG (Caspase-3)	1	-6.38	20.89	GLU123 THR59 GLY60 TYR204 MET61 HIS121 PHE256
Sitostenone	3ERT (Estrogen receptor alpha)	71	0.41	-	-
	3OLL (Estrogen receptor beta)	17	-7.50	3.2	ALA442, VAL438, SER448
	1A28 (Progesterone receptor)	3	1.79	-	-
	2XYG (Caspase-3)	1	-8.34	770.67	ARG207 MET61 HIS121 CYS163 TYR204
3β-glucose sitosterol	3ERT (Estrogen receptor alpha)	14	1.64	-	ALA551
	3OLL (Estrogen receptor beta)	8	-3.46	2930	ALA A:442, ALA B:442 GLN451, VAL438,
	1A28 (Progesterone receptor)	4	3.88	-	-

(Continued)

**Table 3** (Continued).

Compound	Receptor	Cluster	Binding Energy (kcal/mol)	Ki (μM)	Bond
	2XYG (Caspase-3)	1	−6.94	8.16	ARG207 HIS121 MET61 PHE128
Poriferasta-5,22E,25-trien-3β-ol,22-dehydrocholesterol	3ERT (Estrogen receptor alpha)	62	0.8	-	LEU306
	3OLL (Estrogen receptor beta)	6	−6.52	16.58	ALA442, VAL438, SER452
	1A28 (Progesterone receptor)	17	1.79	-	-
	2XYG (Caspase-3)	1	−7.65	2.46	CYS163 TYR204 HIS121 MET61 PHE128

**Abbreviations:** MCF-7, Michigan Cancer Foundation-7; MDA-MB, M.D. Anderson-Metastasis Breast; mRNA, Messenger RiboNucleic Acid; ESR2, estrogen receptor gene; IC, Inhibitory Concentration; PCR, Polymerase Chain Reaction; RMSD, Root Mean Square Deviation; DNA, Deoxyribonucleic acid; RNA, Ribonucleic acid; Ki, Inhibitor constant. ND, not detected; PDB, protein data bank.

(ALA B: 442, GLN451). Good binding energy and inhibition constant were also reported as −3.46 kcal/mol and 29.5 μM, respectively. Even though 2XYG formed 1 conventional hydrogen bond (ARG207), 1 carbon-hydrogen bond (HIS121), and 2 alkyl bonds (PHE128, MET61) with a binding energy of −6.94 kcal/mol, there was also an inhibition constant of 8.16 μM. In the other 2 receptors, specifically 3ERT and 1A28, the energy was positive, without inhibition constant or receptor binding. The 3OLL receptor showed a negative binding energy of −6.52 kcal/mol and an inhibition constant of 16.58 μM with the compound Poriferasta-5,22E,25-trien-3β-ol,22-dehydrocholesterol. Meanwhile, 2XYG had a binding energy of 7.65 kcal/mol and an inhibition constant of 2.46 μM. The bonds formed were 2 alkyl (ALA442, VAL438) and 1 hydrogen (SER452) while 2XYG had 5 alkyl (MET61, PHE128, HIS121, CYS163, TYR204). At the 1A28 and 3ERT receptors, no binding energy was observed for the tested compounds.

## Apoptotic-Related Gene Signaling mRNA Expression

Apoptotic occurrence and hormone relationship were confirmed through gene signaling of mRNA expression after observing and analyzing data from IC<sub>50</sub> value, cell morphological changes, and molecular docking. The optimal performance was observed with 3β-glucose sitosterol among β-sitosterol derivatives. Therefore, the mechanism of action investigated through PCR focused on 3β-glucose sitosterol on MCF7 cells, serving as a model for estrogen and progesterone hormone-positive breast cancer cell lines. The result of PCR band of apoptotic-related gene mRNA expression is shown in Figure 3. Expression of *caspase-9* and *caspase-3 mRNA* in MCF7 cells treated with 3β-glucose sitosterol after 12 and 24 h gradually increased. Meanwhile, the expression of *Bcl-2* and *PARP-1 mRNA* after treatment with 3β-glucose sitosterol increased slightly and significantly after 12 h and 24 h (Figure 3a-b).

## Estrogen and Progesterone Receptor Gene Signaling mRNA Expression

Morphology cells showed different changes between MCF7 and MDA-MB-231. The distinction was in the hormonal characteristics, where MCF7 and MDA-MB-231 represented estrogen hormone-positive and triple-negative model cells, respectively. However, MCF7 cells showed apoptotic occurrence sign blebbing more than MDA-MB-231. These changes were influenced by the presence of estrogen receptors on MCF7 cells. After the cells were treated with 3β-glucose



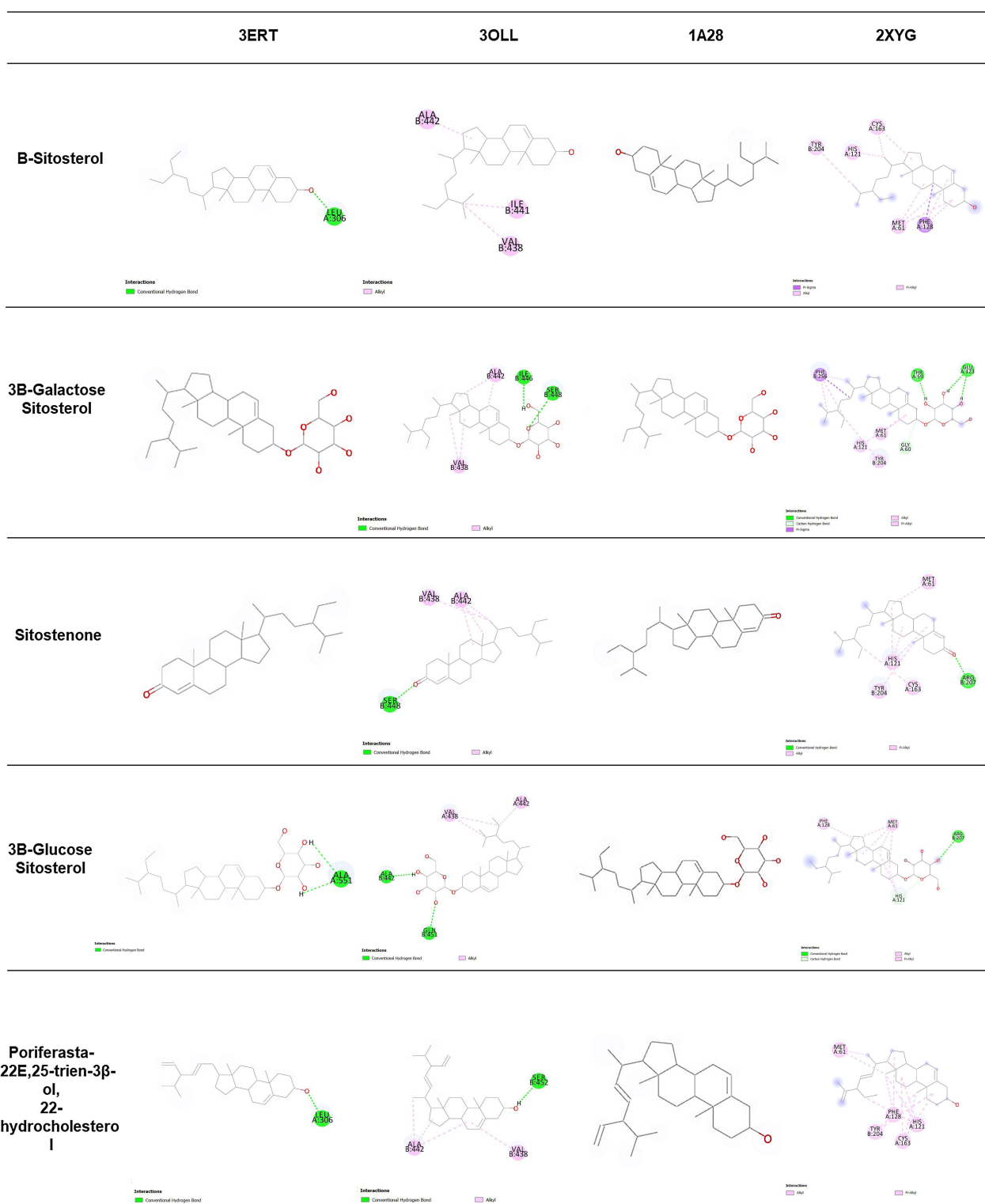


**Figure 2** Ligand-receptors interaction of  $\beta$ -sitosterol compounds and its derivatives against 3ERT, 3OLL, 1A28, and 2XYG receptors.

sitosterol, apoptotic-related gene *mRNA expression* continued to check the estrogen and progesterone receptors (Figure 4a and b).

Figure 4 shows that the expression of estrogen and progesterone in MCF7 increased gradually over time.

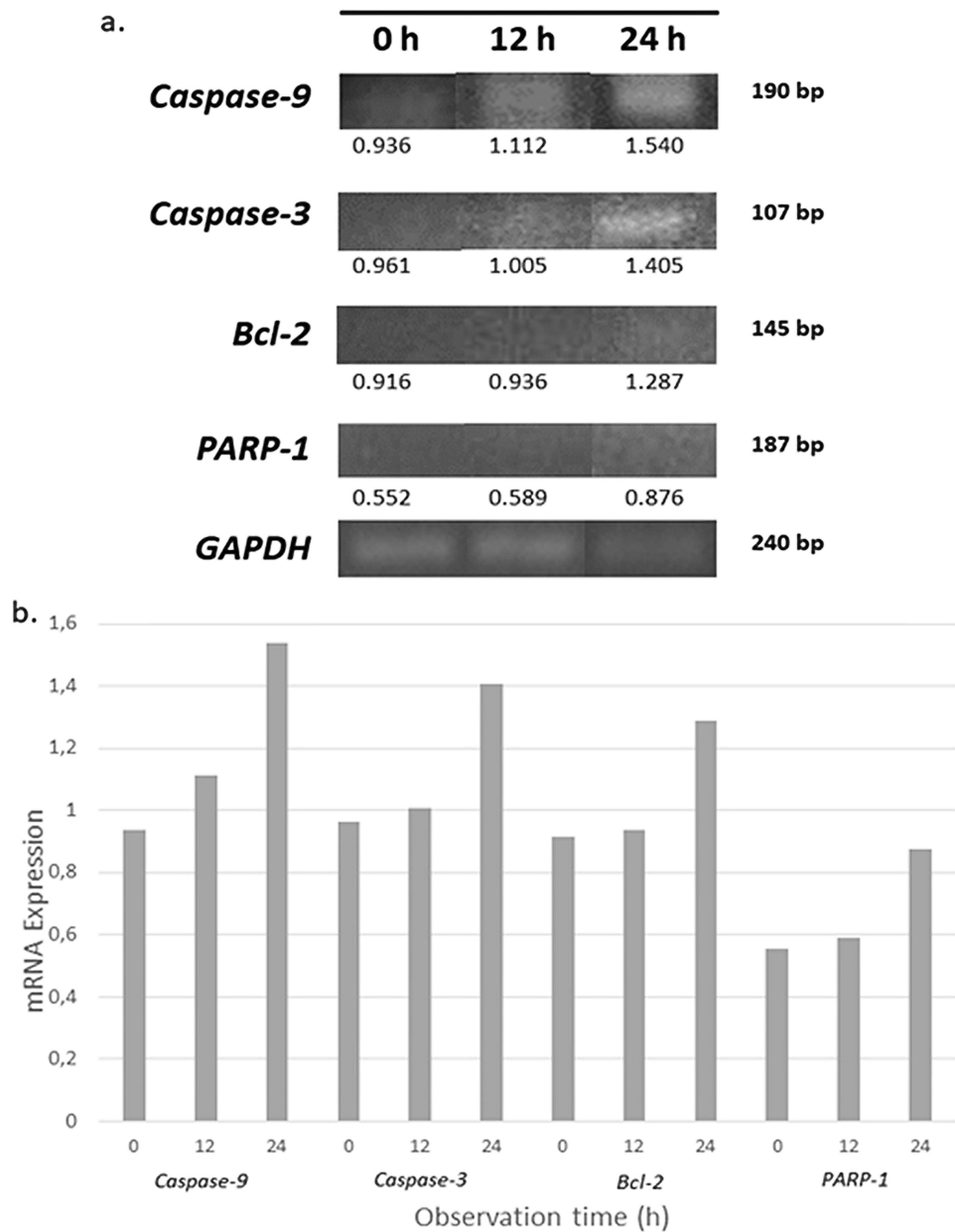


**Figure 3** Apoptotic-related signaling mRNA expression in MCF7 cells treated with 3 $\beta$ -glucose sitosterol (a) The visualization of mRNA expression of caspase-9, caspase-3, Bcl-2, and PARP-1 using electrophoresis gel. Quantitative data of band intensity was measured using ImageJ ver. 1.53e (NIH). (b) Bar graph of mRNA expression of caspase-9, caspase-3, Bcl-2, and PARP-1 obtained by RT-PCR in MCF7 cells treated with 3 $\beta$ -glucose sitosterol. One-way ANOVA followed by Tukey's post hoc test was performed when  $p < 0.05$ .

## Discussion

Breast cancer is a serious malignant disease, becoming the most frequently diagnosed worldwide. Combination therapy is often used for patients with breast cancer, with hormone being one of the considered methods. Investigating the potential for use in assisting patients remains important since there are plant materials whose benefits remain unexplored.<sup>16</sup> Phytosterol is abundant in plant sources but has not been studied for breast cancer. Beta-Sitosterol and the 4 derivatives, 3 $\beta$ -galactose sitosterol, sitostenone, 3 $\beta$ -glucose sitosterol, poriferasta-5,22E,25-trien-3 $\beta$ -ol,22-dehydrocholesterol, were tested on MCF7 and MDA-MB-231, as well as on MCF 10A as non-cancerous breast epithelial cells. This study has potential limitations. The reliance on MCF7 and MDA-MB-231 cell lines may not fully capture the complexity of human breast tumors, and the long-term effects of treatment remain unexplored.

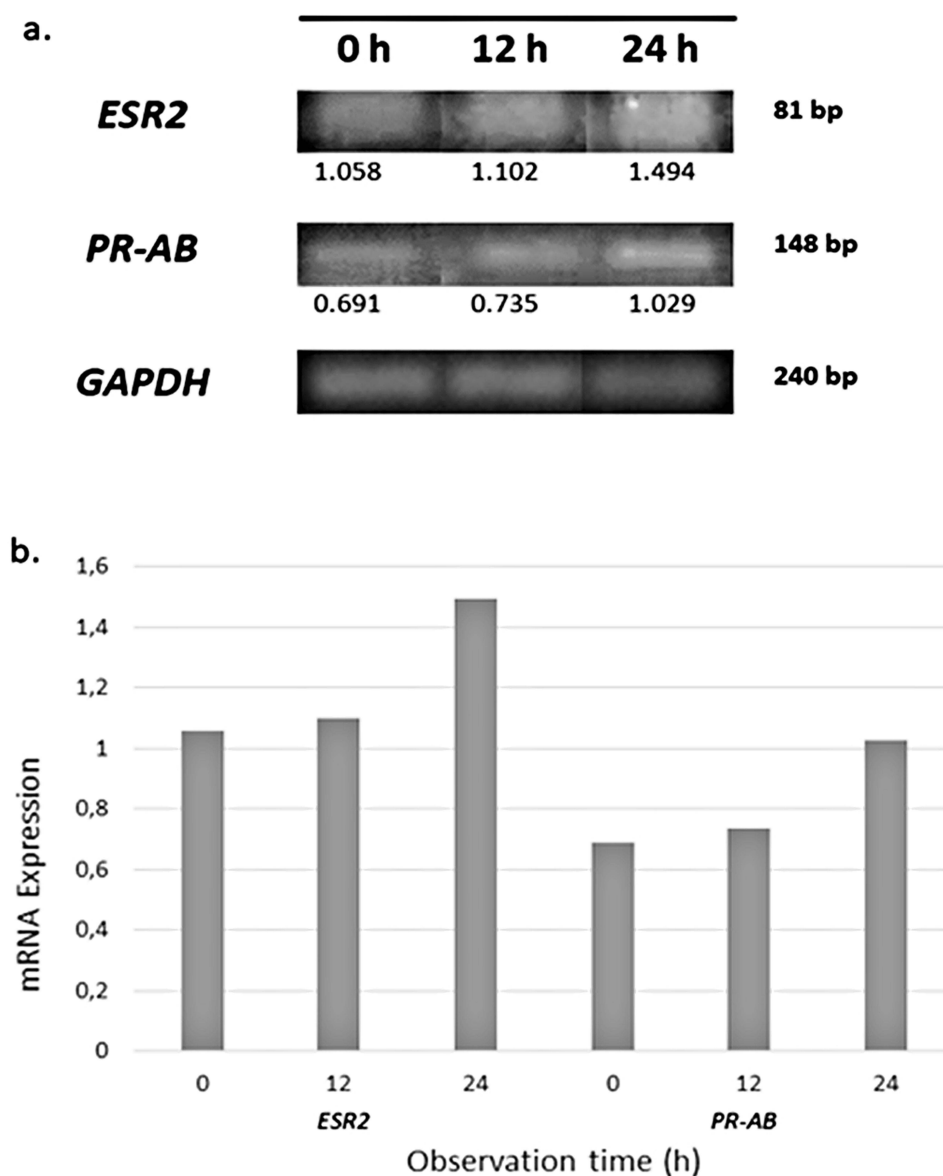


**Figure 4** Estrogen and progesterone mRNA expression in MCF7 cells treated with 3 $\beta$ -glucose sitosterol (a) The visualization of mRNA expression of ESR2, estrogen, and PR-AB progesterone using electrophoresis gel. Quantitative data of band intensity was measured using ImageJ ver. 1.53e (NIH). (b) Bar graph of mRNA expression of ESR2 and PR-AB obtained by RT-PCR in MCF7 cells treated with 3 $\beta$ -glucose sitosterol. One-way ANOVA followed by Tukey's post hoc test was performed when  $p < 0.05$ .

The criteria used to categorize the cytotoxicity of  $\beta$ -sitosterol and its derivatives based on US National Cancer Institute (NCI) and Geran's protocol were as follows:  $IC_{50} \leq 20 \mu\text{g/mL}$  = highly cytotoxic,  $IC_{50}$  ranged between 21 and 200  $\mu\text{g/mL}$  = moderately cytotoxic,  $IC_{50}$  ranged between 201 and 500  $\mu\text{g/mL}$  = weakly cytotoxic and  $IC_{50} > 501 \mu\text{g/mL}$  = not cytotoxicity.<sup>17</sup> The selective cytotoxic compound is 3 $\beta$ -glucose sitosterol, showing  $IC_{50}$  values of 265  $\mu\text{g/mL}$  and 393.862  $\mu\text{g/mL}$ , which include weak cytotoxic against MCF7 and MDA-MB-231 breast cancer cells, respectively. Meanwhile, the  $IC_{50}$  value against MCF 10A non-cancerous cells indicated no cytotoxicity, with a value of 806.833  $\mu\text{g/mL}$ , as reported in Table 2. The morphological changes observed in MCF7 treated with 3 $\beta$ -glucose and 3 $\beta$ -galactose sitosterol appeared to show a higher occurrence of apoptosis compared to cells treated with only  $\beta$ -sitosterol. Previous studies have shown that the sugar moiety in 3 $\beta$ -glucose sitosterol ( $\beta$ -sitosterol-3-O- $\beta$ -D-glucopyranoside) plays a crucial role in enhancing drug absorption by improving solubility and stability, facilitating transport across intestinal membranes via glucose transporters, and protecting the compound from rapid metabolism, which collectively lead to increased bioavailability; additionally, it contributes to cytotoxicity through its antioxidant properties and the ability to selectively

target cancer cells by modulating key signaling pathways involved in cell growth and apoptosis, thereby optimizing its therapeutic potential.<sup>18</sup> Molecular docking tests were performed against 3ERT, 3OLL, 1A28, and Caspase-3 (2XYG).  $\beta$ -Sitosterol reported a favorable binding energy of  $-6.14$  kcal/mol to 3OLL and an inhibition constant of  $31.81$   $\mu$ M. Similarly, the 2XYG receptor also manifested a positive binding energy value of  $-7.98$  kcal/mol and an inhibition constant of  $1.41$   $\mu$ M. The other receptors showed positive binding energy and lacked inhibition constant. In the compound  $3\beta$ -galactose sitosterol, the binding energy and inhibition constant were reported for the estrogen receptor beta ( $-3.31$  kcal/mol,  $3720$   $\mu$ M) and caspase 3 ( $-6.38$  kcal/mol,  $20.89$   $\mu$ M). Sitostenone manifested strong binding energy ( $-7.50$ ;  $-8.34$  kcal/mol) towards 3ERT and Caspase-3 with inhibition constants of  $3.2$  and  $770.67$   $\mu$ M, respectively. Similarly, 3OLL and 2XYG also reported binding energy of  $-3.46$  kcal/mol and  $-6.94$  kcal/mol towards  $3\beta$ -glucose sitosterol accompanied by inhibition constants of  $2930$  and  $-6.94$   $\mu$ M, respectively. Poriferasta-5,22E,25-trien- $3\beta$ -ol,22-dehydrocholesterol showed negative binding energy ( $-6.52$  kcal/mol) and an inhibition constant of  $16.58$   $\mu$ M, where 3OLL and 2XYG reported values of  $-7.65$  kcal/mol and  $2.46$   $\mu$ M, respectively. However, there was no binding at the progesterone and estrogen receptor alpha for any of the tested compounds. Apoptotic-related genes as well as estrogen and progesterone receptors of apoptosis primer were designed to confirm the molecular mechanism of  $3\beta$ -glucose sitosterol to MCF7 cells. The results confirmed the occurrence of apoptosis with the upregulated *caspase-9* and *3* mRNA expression, while *Bcl-2* and *PARP-1* mRNA expression were slightly increased during 24 h (Figure 2).

The morphology result showed that most cells experienced apoptosis in MCF7 given  $3\beta$ -glucose sitosterol (Figure 1K). Meanwhile, with Sitostenone, MCF7 cells experienced a decrease in number but was not an apoptotic process. This was because the cells did not experience blebbing or cell debris (Figure 1H). Likewise, MDA-MB-231 cells exposed to Sitostenone also experienced a decrease in number but were not apoptotic (Figure 1). In MCF 10A, there were no significant morphological changes when exposed to  $3\beta$ -glucose sitosterol or Sitostenone (Figure 1G and J). There are incongruent results between proliferation and cell morphology observations. According to the hypothesis,  $\beta$ -sitosterol derivatives containing sugar groups should have a better cytotoxic effect because of increased level of solubility and cell absorbance. The  $IC_{50}$  value did not decrease despite the observed cell death, particularly in MCF7 exposed to  $3\beta$ -glucose sitosterol (Figure 1K). The results show that the resazurin dye binds to the sugar groups resulting from cell metabolism to change the color to resofurin.<sup>19</sup> In this research, resazurin binds to the sugar group of the tested compound, converting into resofurin, which produces a constant pink color. Therefore, the color change reaction is caused by the bonding of resazurin with the sugar group in the structure of  $\beta$ -sitosterol derivative compound. In this context, the  $IC_{50}$  value of  $\beta$ -sitosterol derivative compounds with sugar groups is large even though almost all cells die from the morphology results. Figure 1 shows that MCF7 cells experience more apoptosis than MDA-MB-231. This is because MCF7 is a cell model for breast cancer cells with estrogen and progesterone receptors. According to predictions, the molecular bond simulation is reported using molecular docking to determine the working mechanism of the  $\beta$ -sitosterol derivative compound.

Table 3 presents molecular tethering for 5  $\beta$ -sitosterol compounds and derivatives against 4 receptors, namely 3ERT, 3OLL, 1A28, and 2XYG. Among these compounds, the most promising results were obtained against the 3OLL and 2XYG receptors. The binding energy values observed for these receptors were notably low ( $-6.14$  to  $-7.98$  kcal/mol). Lower binding energy values indicate stronger interactions between the ligand and the receptor.<sup>20</sup> The assessment of binding energy serves as a critical indicator of the potential efficacy of these compounds in therapeutic applications. Values below  $-5$  kcal/mol are generally accepted as indicative of significant receptor–ligand interactions.<sup>21</sup> In this study, the inhibition constant ( $K_i$ ) values further elucidate the potency of these interactions, with lower  $K_i$  values suggesting a greater inhibitory capacity on receptor activity. A smaller  $K_i$  value shows a lower concentration of ligand required to inhibit receptor activity.<sup>22</sup> In addition, two receptors manifested inhibition constant values for the 5 compounds, namely 3OLL ( $31.81$ ,  $3270$ ,  $3.2$ ,  $2930$ , and  $16.58$   $\mu$ M) and 2XYG ( $1.41$ ,  $20.89$ ,  $770.67$ ,  $8.16$ , and  $2.46$   $\mu$ M). The remaining receptors did not have a  $K_i$  value showing no inhibition ability. The interaction mechanisms identified—hydrogen bonds and van der Waals interactions—are essential in receptor–ligand dynamics. Specifically, the presence of multiple hydrogen bonds in the 2XYG receptor enhances its binding affinity, thereby suggesting a more favorable interaction profile for  $\beta$ -sitosterol derivatives.<sup>23</sup> The 3OLL receptor showed the presence of hydrogen bonds and alkyl bonds. Conversely, the 2XYG receptor had more bonds including conventional hydrogen, alkyl, pi-alkyl, and carbon-hydrogen.



In this context, 3OLL and 2XYG receptors reported smaller binding energies and inhibitory marker values. The result showed that 5  $\beta$ -sitosterol compounds and derivatives could bind and interact with 3OLL and 2XYG to provide antiproliferative effects and serve as mediators of apoptosis, respectively.

Verification with marker genes is important to prove the mechanism of decreasing cell numbers due to programmed death. The marker used is apoptotic-related gene *caspase-9*, which acts as an inducer of apoptosis. The density band calculations reported that there was an increase in *caspase-9* gene expression in MCF7 cells treated with 3 $\beta$ -glucose sitosterol (Figure 3a). Therefore, *caspase-9* induced apoptosis as evidenced by an increase in the executor gene expression within 24 h (Figure 3a). In the *mRNA expression* of the *BCl2* and *PARP-1*, there was a slight increase in gene expression (Figure 3). This was because of the apoptosis but the process was not completed within the observation period of 24 h. In previous results, the expected mechanism of action for antitumor agents was programmed cell death.<sup>24</sup> From cell morphology and predictions using molecular docking, this programmed death was induced by binding to estrogen and progesterone receptors. Therefore, an examination was carried out using gene expression through PCR. The results showed that the expression of *ESR2* and *PR-AB* corresponded to *caspase-9* functioning to induce *caspase-3* (Figures 3a and 4a). According to,<sup>25</sup> the increase in *caspase 3* and *9* gene expression was accompanied by *ESR2* estrogen and *PR-AB* progesterone receptor genes.

Further research should include in vivo formulation, clinical analyses, and another pathway mechanism on 3 $\beta$ -glucose sitosterol. This allows 3 $\beta$ -glucose sitosterol to potentially serve as an adjuvant therapy for breast cancer patients with positive estrogen and progesterone types resulting from hormonal imbalances.

## Conclusion

In conclusion, the study analyzed the cytotoxic activity of  $\beta$ -sitosterol and its derivatives against breast cancer cells MCF7 and MDA-MB-231, compared to non-cancerous cells MCF 10A. The results showed that 3 $\beta$ -glucose sitosterol exhibited the highest cytotoxic effect with IC<sub>50</sub> values of 265  $\mu$ g/mL against MCF-7, 393.862  $\mu$ g/mL against MDA-MB-231, and 806.833  $\mu$ g/mL against MCF 10A cells. This is supported by in silico analysis, in which 3 $\beta$ -glucose sitosterol indicated strong binding energy of -6.94 kcal/mol and inhibition constant 8.16  $\mu$ M to caspase-3 receptors and -3.31 kcal/mol and 3720  $\mu$ M to receptor estrogen beta, further supporting their potential as antiproliferative agents. Gene expression analysis confirmed the mechanism of action through the upregulation of apoptotic-related genes and estrogen/progesterone receptors. Overall, 3 $\beta$ -glucose sitosterol shows the most promising potential adjuvant therapy for hormone-positive breast cancer, emphasizing the need for further research with a broader range of breast cancer cell lines, including hormone receptor-negative cells, in vivo, formulation, clinical analyses and another pathway mechanism on 3 $\beta$ -glucose sitosterol.

## Highlight

- Morphology showed most cell apoptosis in MCF7 given 3 $\beta$ -glucose sitosterol
- Sitostenone showed the biggest cytotoxic effect on MCF-7 cells (IC<sub>50</sub>:168,52  $\mu$ g/mL)
- $\beta$ -sitosterol and derivatives interact well with estrogen receptor beta and caspase-3
- 3 $\beta$ -glucose sitosterol on MCF7 cells mechanism: upregulated *caspase-9* and *3 mRNA*

## Acknowledgments

The authors are grateful to Ms. Hanny Nugrahani for technical support.

## Funding

This research was supported by the Internal Research Grant of Universitas Padjadjaran for sponsoring the research (Hibah Riset Unpad) under number 1549/UN6.3.1/PT.00/2023.

## Disclosure

The authors report no conflicts of interest in this work.

## References

1. Brown JS, Amend SR, Austin RH, Gatenby RA, Hammarlund EU, Pienta KJ. Updating the definition of cancer. *mol Cancer Res.* **2023**;21(11):1142–1147. doi:10.1158/1541-7786.MCR-23-0411
2. Bray F, Laversanne M, Sung H, et al. Global cancer statistics 2022: GLOBOCAN estimates of incidence and mortality worldwide for 36 cancers in 185 countries. *CA Cancer J Clin.* **2024**;74(3):229–263. doi:10.3322/caac.21834
3. Agostinetti E, Gligorov J, Piccart M. Systemic therapy for early-stage breast cancer: learning from the past to build the future. *Nat Rev Clin Oncol.* **2022**;19(12):763–774. doi:10.1038/s41571-022-00687-1
4. Talib WH, Alsayed AR, Barakat M, Abu-Taha MI, Mahmood AI. Targeting drug chemo-resistance in cancer using natural products. *Biomedicines.* **2021**;9(10). doi:10.3390/biomedicines9101353
5. Lee AV, Oesterreich S, Davidson NE. MCF-7 cells—changing the course of breast cancer research and care for 45 years. *J Natl Cancer Inst.* **2015**;107(7):djv073. doi:10.1093/jnci/djv073
6. Kotta-Loizou I, Vasilopoulos SN, Coutts RH, Theocharis S. Current evidence and future perspectives on HuR and breast cancer development, prognosis, and treatment. *Neoplasia.* **2016**;18(11):674–688. doi:10.1016/j.neo.2016.09.002
7. Pascut D, Pratama MY, Vo NVT, Masadah R, Tiribelli C. The crosstalk between tumor cells and the microenvironment in hepatocellular carcinoma: the role of exosomal microRNAs and their clinical implications. *Cancers.* **2020**;12(4):1–20. doi:10.3390/cancers12040823
8. Tahsin T, Wansi JD, Al-Groshi A, et al. Cytotoxic properties of the stem bark of *Citrus reticulata* Blanco (Rutaceae). *Phytother Res.* **2017**;31(8):1215–1219. doi:10.1002/ptr.5842
9. Wahyuni W, Diantini A, Ghazali M, et al. In-vitro anticancer activity of chemical constituents from *Etlingera alba* Poulsen against triple negative breast cancer and in silico approaches towards matrix metalloproteinase-1 inhibition. *Indonesian J Sci Technol.* **2022**;7:251–278. doi:10.17509/ijost.v7i2.50547
10. Bao X, Zhang Y, Zhang H, Xia L. Molecular mechanism of  $\beta$ -sitosterol and its derivatives in tumor progression. *Front Oncol.* **2022**;12:926975. doi:10.3389/fonc.2022.926975
11. Hadisaputri YE, Andika R, Sopyan I, et al. Caspase cascade activation during apoptotic cell death of human lung carcinoma cells A549 induced by marine sponge *Callyspongia aerizusa*. *Drug Des Devel Ther.* **2021**;15:1357–1368. doi:10.2147/DDDT.S282913
12. Decloedt AI, Van Landschoot A, Watson H, Vanderputten D, Vanhaecke L. Plant-based beverages as good sources of free and glycosidic plant sterols. *Nutrients.* **2017**;10(1):21. doi:10.3390/nu10010021
13. Chowdhury R, Rashid RB, Sohrab MH, Hasan CM. 12 $\alpha$ -hydroxystigmast-4-en-3-one: a new bioactive steroid from *Toona ciliata* (Meliaceae). *Pharmazie.* **2003**;58(4):272–273. doi:10.1002/chin.200332126
14. Musa W, Hersanti H, Zainuddin A, ati TR. The poriferasta compound-5,22E,25-TRIEN-3-O $\beta$  from *Clerodendrum paniculatum* leaf as inducer agent of systemic resistance on red chilli plant *Capsicum annuum* L from cucumber mosaic virus (CMV). *Indones J Chem.* **2010**;9:487–490. doi:10.22146/ijc.21521
15. Wiji Prasetyaningrum P, Bahtiar A, Hayun H. Synthesis and cytotoxicity evaluation of novel asymmetrical mono-carbonyl analogs of curcumin (AMACs) against Vero, HeLa, and MCF7 cell lines. *Sci Pharm.* **2018**;86(2):25. doi:10.3390/scipharm86020025
16. Łukasiewicz S, Czezelewski M, Forma A, Baj J, Sitarz R, Stanisławek A. Breast cancer-epidemiology, risk factors, classification, prognostic markers, and current treatment strategies-an updated review. *Cancers.* **2021**;13(17):4287. doi:10.3390/cancers13174287
17. Geran RI, Greenberg NH, MacDonald MM, Schumaker AM, Abbott BJ. Protocols for screening chemical agents and natural products against animal tumors and other biological systems. *Cancer Chemother Rep.* **1972**;3:59–61.
18. Afifi S, Sherif M, Kamel R, Esatbeyoglu T, Hassan H.  $\beta$ -sitosterol glucoside-loaded nanosystem ameliorates insulin resistance and oxidative stress in streptozotocin-induced diabetic rats. *Antioxidants.* **2022**;11(5):1023. doi:10.3390/antiox11051023
19. Paul M, Strassl F, Hoffmann A, Hoffmann M, Schlüter M, Herres-pawlis S. Aspects of bubbly flows for chemists | very important paper | reaction systems for bubbly flows. 2101–2124. doi:10.1002/ejic.201800146.
20. Du X, Li Y, Xia YL, et al. Insights into protein-ligand interactions: mechanisms, models, and methods. *Int J mol Sci.* **2016**;17(2):144. doi:10.3390/ijms17020144
21. Rena SR, Nurhidaya N, Rustan R. Analisis Molecular Docking Senyawa Garcinia mangostana L Sebagai Kandidat Anti SARS-CoV-2. *Jurnal Fisika Unand.* **2022**;11(1):82–88. doi:10.25077/jfu.11.1.82-88.2022
22. Puspita PJ, Liliyani NPP, Ambarsari L. Potential of active compounds in leaves, seeds, and peel of avocado fruit (*Persea americana* Mill.) as in silico tyrosinase enzyme inhibitors. *Curr Biochem.* **2022**;9(2):73–87. doi:10.29244/cb.9.2.3
23. Frimayanti N, Lukman A, Nathania L. Studi molecular docking senyawa 1,5-benzothiazepine sebagai inhibitor dengue DEN-2 NS2B/NS3 serine protease. *Chempublish J.* **2021**;6(1):54–62. doi:10.22437/chp.v6i1.12980
24. Hadisaputri YE, Habibah U, Abdullah FF, et al. Antiproliferation activity and apoptotic mechanism of soursop (*Annona muricata* L.) leaves extract and fractions on MCF7 breast cancer cells. *Breast Cancer (Dove Med Press).* **2021**;13:447–457. doi:10.2147/BCTT.S317682
25. Chimento A, De Luca A, Avena P, et al. Estrogen receptors-mediated apoptosis in hormone-dependent cancers. *Int J mol Sci.* **2022**;23(3):1242. doi:10.3390/ijms23031242

**Journal of Experimental Pharmacology****Publish your work in this journal**

The Journal of Experimental Pharmacology is an international, peer-reviewed, open access journal publishing original research, reports, reviews and commentaries on all areas of laboratory and experimental pharmacology. The manuscript management system is completely online and includes a very quick and fair peer-review system. Visit <http://www.dovepress.com/testimonials.php> to read real quotes from published authors.

Submit your manuscript here: <https://www.dovepress.com/journal-of-experimental-pharmacology-journal>

**Dovepress**  
Taylor & Francis Group